



Published in final edited form as:

Neuroimage. 2017 August 15; 157: 545–554. doi:10.1016/j.neuroimage.2017.06.014.

Instantaneous Voltage as an Alternative to Power- and Phase-Based Interpretation of Oscillatory Brain Activity

Gerwin Schalk^{1,2,3,*}, Joshua Marple^{1,4}, Robert T. Knight⁵, and William G. Coon^{1,6}

¹National Center for Adaptive Neurotechnologies, Wadsworth Center, New York State Dept. of Health, Albany, NY

²Dept. of Neurology, Albany Medical College, Albany, NY

³Dept. of Biomedical Sciences, State University of New York, Albany, NY

⁴Dept. of Computer Science, University of Kansas, Lawrence, KS

⁵Dept. of Psychology and the Helen Wills Neuroscience Institute, University of California at Berkeley, Berkeley, CA

⁶Dept. of Psychiatry, Massachusetts General Hospital, Harvard Medical School, Boston, MA

Abstract

For decades, oscillatory brain activity has been characterized primarily by measurements of power and phase. While many studies have linked those measurements to cortical excitability, their relationship to each other and to the physiological underpinnings of excitability is unclear. The recently proposed Function-through-Biased-Oscillations (FBO) hypothesis [1] addressed these issues by suggesting that the voltage potential at the cortical surface directly reflects the excitability of cortical populations, that this voltage is rhythmically driven away from a low resting potential (associated with depolarized cortical populations) towards positivity (associated with hyperpolarized cortical populations). This view explains how oscillatory power and phase together influence the instantaneous voltage potential that directly regulates cortical excitability. This implies that the alternative measurement of instantaneous voltage of oscillatory activity should better predict cortical excitability compared to either of the more traditional measurements of power or phase. Using electrocorticographic (ECoG) data from 28 human subjects, the results of our study confirm this prediction: compared to oscillatory power and phase, the instantaneous voltage explained 20% and 31% more of the variance in broadband gamma, respectively, and power and phase together did not produce better predictions than the instantaneous voltage. These results synthesize the previously separate power- and phase-based interpretations and associate oscillatory activity directly with a physiological interpretation of cortical excitability. This alternative view has implications for the interpretation of studies of oscillatory activity and for current theories of cortical information transmission.

* gschalk@neurotechcenter.org.

Publisher's Disclaimer: This is a PDF file of an unedited manuscript that has been accepted for publication. As a service to our customers we are providing this early version of the manuscript. The manuscript will undergo copyediting, typesetting, and review of the resulting proof before it is published in its final citable form. Please note that during the production process errors may be discovered which could affect the content, and all legal disclaimers that apply to the journal pertain.

Introduction

A central goal of neuroscience is to determine how the relatively static anatomy of the brain can support dynamic cortical function, i.e., cortical function that varies according to rapidly changing task demands. Ever since seminal studies in the 1930s [2], it has become increasingly recognized that low-frequency oscillatory activity plays an important role in dynamically modulating the activity of the cortex. However, exactly how oscillations may serve this purpose, and how to best measure their modulatory effect has been debated.

Current understanding of the functional significance of oscillatory activity is based on a large number of studies that have linked oscillatory activity to *cortical excitability*, i.e., the probability of action-potential firing or its macroscopic correlates, and to resultant variations in behavioral performance. While there is still debate about the generators of oscillatory activity, substantial evidence points to interactions between subcortical and cortical structures. For example, for oscillations in the alpha band, studies have repeatedly implicated specific thalamic nuclei and corresponding cortical areas [3, 4]. At the same time, how the properties of such oscillations should best be measured using macroscopic recording techniques (e.g., electrocorticography (ECoG), electroencephalography (EEG), or magnetoencephalography (MEG)) is not clear. Macroscopic measurements are influenced by many factors that include the directional orientation of cortical neurons to each other and to the recording electrode, or the location of the referencing electrode with respect to the recording electrode. Because the precise anatomical and geometric relationships are generally not available for large populations of neurons, it has not been feasible to establish generalized biophysical models of oscillatory activity that is measured at a specific cortical location¹. Thus, while theoretically possible, the limitations of current technologies make it impractical to use biophysical models to describe how oscillatory activity manifests in specific macroscopic recordings, and to use this information to inform signal processing algorithms that extract relevant aspects of oscillatory activity from those recordings.

In spite of this limitation, many experimental studies have demonstrated relationships between specific features of oscillatory activity and cortical function. These studies suggest that the power or phase of oscillatory activity modulates the level of cortical activity or behavioral performance [6, 7, 8, 9, 10, 11, 12, 13, 14, 15, 16, 17, 18, 19, 20, 21, 22, 23, 24, 25, 26, 27, 28, 29, 30, 31, 32] and hence plays a central role in the dynamic modulation of cortical function in response to varying task demands [33, 34, 35]. Specifically, these and other studies have consistently reported that during times when oscillatory power is low or during times of an oscillatory trough, the probability of action potential firing rate, broadband gamma augmentation, or higher behavioral performance is increased².

¹Biophysical models can be very powerful tools for interpretation and simulation. At the same time, they are also subject to important constraints. For example, neural-biophysical models frequently only describe the activity of very specific and well-defined circuits, and their validity may not generalize beyond one or a few specific brain states (e.g., models that describe electrical/neural behavioral during non-rapid eye movement (NREM) sleep, but not during REM or wakefulness; see [5] for an example). They currently certainly cannot give a mathematical formulation of an oscillation that we may observe in one specific ECoG recording location.

²This consistency is interesting since we are well aware that the amplitude and even polarity of an electrophysiological signal critically depends on the location of the reference electrode.

In contrast to low-frequency oscillatory activity, many studies have suggested that the key indicator of cortical population-level activity (i.e., *cortical excitation*) is ECoG activity in the broadband gamma (70–170 Hz) range [36, 27, 37, 38, 39, 40, 41, 42, 43, 44, 45, 46]. Broadband gamma has been shown to be a direct reflection of the average firing rate of neurons directly underneath the electrode [47, 48, 49, 50], and has been shown to drive the BOLD signal identified using fMRI [51, 52, 53, 54]. The physiological underpinnings of broadband gamma are that of a non-oscillatory noise process that is best captured by measurements of power, variance, or voltage envelope [47, 48, 49, 50].

Despite the number and consistency of the reports relating oscillatory power and phase to cortical excitability, it is important to recognize that the specific choice of each of these two measurements is arbitrary and not informed by biophysical or physiological principles. This situation creates two important issues that have not received much attention. First, the choice of these measurements and the methods to extract them are based on assumptions about the characteristics of oscillatory activity that are imprecise. For example, the measurement of the power or phase in a signal using the Fast Fourier Transformation (FFT) or other prevalent techniques is based on the assumption that oscillatory activity is sinusoidal in shape and varies symmetrically about a mean. However, it is well known that oscillatory activity is not sinusoidal [55, 56, 57, 58], and there have been initial experimental reports [59, 60] that described asymmetric voltage distributions in oscillatory activity. The second important issue is that it is unclear why cortical excitability appears to be related to two mathematically independent measurements (power and phase) of the same physiological process. In summary, the current lack of a formal model of oscillatory activity and the issues with current methods to extract measurements from them impedes the physiological interpretation of experimental findings involving oscillatory activity, and results in suboptimal measurements of cortical excitability.

The recently formalized Function-through-Biased-Oscillations (FBO) hypothesis [1] describes an alternative view that addresses both issues. Synthesizing results from single-neuron neurophysiological studies [61] and other contributions [62, 58], the first principle of the FBO hypothesis suggests that oscillatory activity may best be conceptualized as rhythmic inhibition of neuronal populations in the cortex that may be produced by rhythmically discharging neurons in subcortical nuclei. In this view, macroscopic voltage measurements reflect a low resting voltage at which cortical neurons are depolarized; the rhythmic arrival of subcortical action potential volleys moves the detected voltage toward and away from positivity, thereby rhythmically hyperpolarizing/inhibiting the cortical populations. This rhythmic inhibition creates an asymmetric voltage distribution similar to that shown by the yellow trace in the top right panel of Fig. 1. This working hypothesis does not describe a biophysical but rather a physiologically inspired model of oscillatory activity. At the same time, it suggests a plausible description for the physiological mechanism underlying rhythmic voltage changes at the cortical surface and provides an approach to optimize the extraction of measurements of cortical excitability.

This view is also consistent with the existing experimental findings based on oscillatory power or phase (see Fig. 1, top panel, green and blue traces on the left and center, respectively). On average, cortical excitability is high for small values of oscillatory power

(the left part of the green trace, also see green trace in center panel), and for the trough of oscillatory phase ($\pm\pi$, see blue trace in center panel). It is also apparent that the predictions based on oscillatory power and phase can sometimes contradict each other. For example, low oscillatory power should predict a relatively constant high level of cortical excitability, but the peak/trough phases within the same periods should predict variable levels of excitability. Also see Fig. 4 in [1].

If this central proposal of the FBO hypothesis is correct, the variations in instantaneous voltage amplitude of biased oscillations (as shown in the yellow trace in the top panel in Fig. 1) should most directly relate to variations in cortical excitability. This view provides an alternative to power/phase-based conceptualization of oscillations that is simpler (one measurement instead of two) and more physiologically plausible (as it can readily be conceptualized by voltage deviations caused by subcortical action potential volleys). More importantly in the context of the present study, it also creates two important and testable predictions: 1) the instantaneous voltage of biased oscillations is a better predictor of cortical excitability than either oscillatory power or phase; and 2) oscillatory power and phase together should not predict excitability better than the instantaneous voltage. The study described in this paper confirms these predictions.

Materials and Methods

Subjects and Data Collection

We recorded ECoG signals from 28 human epilepsy patients who each had 58–134 ECoG electrodes (2,442 total) implanted for the purpose of presurgical planning. Recording was accomplished at the bedside using the general-purpose BCI2000 software [63, 64], which interfaced with eight 16-channel g.USBamp biosignal acquisition devices or a single 256-channel g.HIamp biosignal acquisition device (g.tec, Graz, Austria). A splitter box routed signals simultaneously to the clinical monitoring system and to the BCI2000/amplifier system, and thereby supported continuous clinical monitoring. The signals were amplified, digitized at 1200 Hz, and stored by BCI2000. Electrode contacts distant from epileptic foci and areas of interest were used for reference and ground.

Behavioral Task

Each subject performed in three conditions: 1) alternating sequences of repetitive movements of the hand (manipulating a Rubik's cube) or orofacial muscles (protruding and retracting the tongue or lips); 2) passive listening (short stories presented with computer speakers); and 3) periods of rest. In each trial, BCI2000 cued the subject visually to the task by presenting the words "solve Rubik's cube," "stick out tongue," "kiss," "listen carefully," or "stop and relax." Each task was performed for 15 seconds (except for passive listening, which was 17–36 seconds depending on which narrative was presented). The motor tasks were performed at a self-paced rate of about two repetitions per second. Each task was followed by a resting period of 15 seconds before the next task proceeded. One run consisted of 5 repetitions of this sequence over the course of 10.22 minutes (4.75 minutes rest, 1.25 minutes hand moving, 1.25 minutes tongue moving, 1.25 minutes lips moving, and 1.72 minutes passive listening). We typically recorded one initial run to familiarize the subject

with the task. This initial run was not included in data analyses. To test the main hypotheses in our study on two spatially and functionally distinct brain networks, we focused the analyses described here on the data from the hand movement, passive listening, and resting periods.

Data Preprocessing

Before proceeding with analyses, we inspected ECoG recordings visually offline, and removed from further analyses those channels that did not contain clear ECoG signals (e.g., ground/reference channels, channels with broken connections, presence of environmental artifacts, or interictal activity). In addition, we excluded channels with excessive line noise. To identify those channels, we first applied an IIR peak filter (MATLAB™ `iirpeak` function) to calculate the signal power at 60 Hz (i.e., line noise) at each channel. Then, across all channels, we calculated the median and the median absolute deviation (MATLAB™ `mad` function) of those line noise values. Finally, we excluded those channels whose 60 Hz line noise value was more than 10 median absolute deviations different from the median line noise. These procedures left 54–132 locations from each subject (2,384 locations total across all subjects) that were submitted to further analysis.

Extraction of Broadband Gamma Activity and Alpha Power/Phase

Testing the main hypotheses in our study required establishing the relationship between three different measurements of cortical excitability and a measurement of cortical excitation. ECoG broadband gamma is widely recognized as a measurement of cortical excitation, because it has been identified as a key indicator of task-related cortical activity in many different experimental paradigms [36, 27, 37, 38, 39, 40, 41, 65, 66, 42, 43, 67, 28, 44, 45, 46]. Moreover, it has been shown to reflect the average firing rate of neurons directly underneath the electrode [68, 48, 49, 50] and has been related to the BOLD signal detected using fMRI [51, 52, 54].

Ever since the discovery of the cortical excitability cycle more than 80 years ago [2], it has been well understood that oscillatory activity is involved in modulating the excitability of neuronal populations in the cortex. The measurements that have usually been made to quantify the magnitude of this modulatory effect are oscillatory power (e.g., [15]) and oscillatory phase (e.g., [19]). Thus, we used those measurements as the two principal traditional indices of cortical excitability.

To extract these features of oscillatory and broadband gamma activity, we first high-pass filtered the ECoG signals at 0.01 Hz and re-referenced them to a common average reference (CAR, [69]). We obtained the CAR-filtered signal s'_h at channel h using the formula

$$s'_h = s_h - \frac{1}{H} \sum_{q=1}^H s_q$$

s_h was the original signal sample at a particular time, and H was all channels included in the CAR. We then extracted the amplitude of oscillatory activity in the alpha band³ (7–12 Hz)

using a 6th order⁴ Butterworth band-pass filter implemented with zero phase lag (MATLAB™ `filtfilt` function), and derived broadband gamma activity by applying a band-pass filter of 70–170 Hz. We then obtained the amplitude envelope (i.e., square root of power) and phase estimates for alpha/gamma activity by applying the Hilbert transform to the respective band-pass filtered time series⁵.

Extraction of Instantaneous Oscillatory Amplitude

We also extracted a novel measurement of oscillatory activity — the instantaneous voltage of oscillatory activity — from the ECoG signals. ECoG voltage measurements are affected not only by oscillatory activity, but also by asynchronous neuronal activity (broadband gamma) or ionic flows (see simulated exemplary noisy voltage trace in Fig. 2-A). Thus, just like with the traditional power and phase measurements derived from oscillatory activity, the instantaneous amplitude of oscillations has to be extracted from the raw ECoG signals to maximally separate it from activity from other sources.

One way to extract the instantaneous amplitude of biased oscillations begins by band-pass filtering oscillatory activity to filter out non-rhythmic activity. This initial step will make the signal zero mean (i.e., it varies symmetrically about zero irrespective of the peak-to-peak amplitude at a particular point in time, Fig. 2-B)⁶. Because the first principle of the FBO hypothesis proposed a model of oscillatory activity in which the troughs of the oscillation are always at the same low voltage level irrespective of the peak-to-peak amplitude, the critical step necessary to derive the instantaneous oscillatory amplitude is to subtract, at each point in time, an estimate of the amplitude bias from the band-pass filtered signal. The resulting signal represents the instantaneous voltage of the biased oscillation (see Fig. 2-C). Thus, the procedure described here is taking advantage of the understanding suggested by the model proposed in the FBO hypothesis.

To calculate the instantaneous voltage amplitude, we first calculated, at each location, the minimum amplitude value of the troughs of each alpha oscillation (i.e., its bias offset, $offset_{bias}$) as the 5th percentile of the voltage values in the band-pass filtered alpha activity time course (see Fig. 2-B). At each point in time, we then derived the amplitude bias as the difference between the negative of the amplitude envelope value, S_{AE} , and the bias offset, $offset_{bias}$, and subtracted it from the band-passed alpha activity value, S_{AA} , to derive a bias-corrected alpha activity value S'_{AA} . See the following equation for the formal definition:

³Oscillations at different frequencies subserve different cortical regions. For example, oscillations in the alpha band are prevalent throughout the sensorimotor system (e.g., Kubanek 2013, Kubanek 2015) and auditory system (e.g., Potes 2012a, Potes 2014). Because the tasks we study here affect neuronal populations in those systems, we focused on alpha oscillations in this study. Please see Discussion for further elaboration.

⁴To ensure that filter order did not present a confound in our analyses, we re-ran our processing pipeline after reducing the filter order to 3, and found no appreciable difference in our results.

⁵The amplitude envelope of an oscillation is the square root of oscillatory power, and so these terms are non-linear versions of each other. While we followed typical ECoG analyses procedures to calculate the envelope of broadband gamma activity (i.e., amplitude), we use the term “oscillatory power” during conceptual presentations of this manuscript to highlight the traditional power/phase framework.

⁶It is important to recognize that, depending on the specific filter coefficients, this bandpass filtering procedure implies a particular shape of rhythmic activity that almost certainly will not match its true shape. Thus, similar to other common approaches to feature extraction, this aspect of our procedure is almost certainly suboptimal.

$$S'_{AA} = S_{AA} - (-S_{AE} - offset_{bias})$$

In summary, this procedure re-introduces the bias that is lost by the bandpass filtering procedure back into the data, and estimates the bias based on a model⁷.

Identification of Task-Related Locations

Evaluating the relationship between specific measurements of cortical excitability and cortical excitation requires that a particular cortical location varies in excitability and excitation throughout the dataset. To ensure this, we selected, in each subject, only those locations for subsequent analyses in which broadband gamma activity changed between rest and one of the two tasks (movement of the hand (i.e., motor task) or passive listening (i.e., auditory task))⁸. We first calculated, separately for each task and location, the pairwise Pearson's coefficient of determination (r^2) between task labels (i.e., task and rest) and broadband gamma activity. To ensure that broadband gamma varied markedly across the dataset (so that we could properly evaluate its relationship with oscillatory activity), we selected from all 2,384 channels only those with r^2 values larger than (the empirical threshold of) 0.2. This yielded 82 task-related locations for the motor task, and 44 different locations for the auditory task. Fig. 3 shows all electrode locations (black dots), the locations that are modulated by the auditory task (44 larger green dots) and motor task (82 larger red dots), for the left (A) and right (B) hemispheres.

Establishing the Relationship between Alpha Power/Phase/Instantaneous Amplitude and Broadband Gamma Activity

Our central question was to determine whether an alternative measure of oscillatory activity, i.e., the instantaneous amplitude, was a better predictor of cortical excitability (as assessed by its proxy broadband gamma) than power or phase. To answer this question, we implemented a procedure that derived, at each location, a measurement of the degree of the relationship between each of the three oscillatory measurements and broadband gamma. Specifically, we fit an appropriate model to the data, determined the fit of the model, and evaluated which of the three models was the best fit for the data across all locations and subjects. The specific procedure that we used to report our primary results is described in more detail in the following section. In addition, we also describe a number of control analyses in a dedicated section "Control Analyses." These additional results address the possibility that the conclusions drawn in this paper were supported by only a small subset of our data or were due to our specific analytical and statistical approach.

Model Fitting and Model Testing

For each location, we established a model that described the relationship between alpha power, phase, or amplitude with broadband gamma activity. Based on preliminary testing,

⁷It is possible to estimate the bias from the measured (unfiltered) signal itself, although there are other sources of low-frequency signal components (e.g., signal drifts due to changes in amplifier characteristics or the electrode interface) that may make this difficult.

⁸Since broadband gamma variations are spatially more focused than are modulations in oscillatory activity (e.g., see [70]), we assume that oscillatory activity at localizations with task-related broadband gamma changes will vary with the task as well.

we used a sigmoid function to model the relationship between alpha power/alpha amplitude and broadband gamma⁹. Based on previous literature [71, 72], we used a cosine function to model the relationship between alpha phase and broadband gamma. See bottom row in Fig. 1 for examples from one electrode location. Similar to Potes et al. [28] and many other studies, broadband power decreases with larger oscillatory power. Similar to Canolty et al. [9] and many other studies, broadband power is also largest during the through of an oscillation.

We used the MatlabTM function `sigm_fit` from the MathWorks FileExchange to establish the sigmoid fits. To ensure that the value range of the x axes for the power and amplitude measurements was not affected by individual outlier samples, we eliminated all samples for which their power/amplitude values were not within their respective 5th–95th percentiles. We used all data for the phase measurement, because phase values are by definition confined to $\pm\pi$. We then binned the samples into 100 linearly spaced bins based on oscillatory power, phase, or instantaneous amplitude, and calculated the mean broadband gamma value in each bin¹⁰.

The distribution of data points may not be even across the range of values of oscillatory power/phase/amplitude. Differences in these distributions may differentially affect the model fits, and thus unfairly favor one model to the other. To eliminate this potential confound, we identified the bin with the smallest number of data points across all three measurements (power/phase/amplitude) within any given channel. We then used this number to subsample data across all bins such that each bin represented the same number of data points, and calculated the three model fits based on these subsampled data populations. We executed this procedure 1000 times using sample-with-replacement, and averaged the results. This procedure resulted in one average measurement of r^2 for each location and for each of the three measurements.

Control Analyses

In the main analyses described in the paper, we used sigmoid and cosine models, and applied them to binned data. In additional control analyses, we used linear and circular-linear models, or applied them to unbinned data. To do this, we computed Pearson's correlation between power or instantaneous voltage and broadband power, and circular-linear correlation (equivalent to Pearson's correlation but with one circular and one linear variable) between phase and broadband power. The circular-linear correlation between a linear variable x and a circular variable a is given by

$$\rho_{cl} = \sqrt{\frac{r_{cx}^2 + r_{sx}^2 - 2r_{cx}r_{sx}r_{cs}}{1 - r_{cs}^2}}$$

⁹As described later, the use of a linear model for establishing these relationships confirmed the principal findings presented here.

¹⁰As described later, the use of other binning methods or no binning method did not alter the principal findings presented here.

where r_{sx} is the Pearson's correlation coefficient between $\sin \alpha$ and x , r_{cx} is the coefficient between $\cos \alpha$ and x , and r_{cs} is the coefficient between $\cos \alpha$ and $\sin \alpha$. These control analyses did not affect our conclusions.

Testing of the First Hypothesis

To test the first and main hypothesis presented in this paper, we determined whether instantaneous amplitude better predicted cortical excitability (as indexed by broadband gamma activity) compared to either the power or the phase. To do this, we compared the distributions of r^2 values (across all of the 44 auditory and 82 motor locations from all subjects) corresponding to fits for power/phase/amplitude to each other (Table 1). To establish these comparisons, we submitted these distributions to a (non-parametric) paired Wilcoxon's Signed Rank test. We also applied the same test to r^2 values derived from all (i.e., not binned) data. Finally, we applied Wilcoxon Signed Rank tests to r^2 values derived from all data points using non-parametric Spearman or circular-linear correlations.

Testing of the Second Hypothesis

If oscillatory power and phase are different reflections of the principal measurement of instantaneous voltage, then oscillatory power and phase together should not predict excitability better than the instantaneous voltage. To test this second hypothesis, we applied the same multi-linear regression analysis to two models. The first model utilized both the amplitude envelope as well as the phase of oscillatory activity. As in Sarma and Jammalamadaka [73], it accounted for the circularity of phase information by incorporating a sine and cosine term and for the sigmoidal relationship between the envelopes of oscillatory activity and broadband gamma by applying a kernel function to transform oscillatory envelope values according to the sigmoid function that was fit to the time series data at that location. The general equation for the model took the form:

$$1. \quad \hat{Y}_t = \hat{\beta}_0 X'_t + \hat{\beta}_1 \cos(\phi_t) + \hat{\beta}_2 \sin(\phi_t) + \hat{\beta}_3$$

where \hat{Y}_t corresponds to the predicted values of broadband gamma envelope, X'_t to the output of the kernel function that transformed oscillatory envelope values, ϕ_t to phase values, and each $\hat{\beta}$ term to successive regression coefficients and a constant offset term. The kernel function, X'_t , took the form:

$$2. \quad X'_t = \frac{a}{1 + e^{(b-x_t) * c}}$$

where a describes the y range (top — bottom) between the sigmoid's asymptotes, b the average of the top and bottom values, c the function's slope, and x_t the original envelope value from that location's time series at time t . Taken together, the final equation for the model can be expressed as:

3.

$$\hat{Y}_t = \hat{\beta}_0 \left(\frac{a}{1 + e^{(b-x_t) * c}} \right) + \hat{\beta}_1 \cos(\phi_t) + \hat{\beta}_2 \sin(\phi_t) + \hat{\beta}_3$$

The second model was set up similarly, but only made use of the instantaneous voltage. It, too, used a sigmoid kernel function to transform the instantaneous voltage time series from each location according to the function parameters determined for those locations in the curve-fitting stage of our procedure. Hence, this equation takes the general form of:

1.

$$\hat{Y}_t = \hat{\beta}_0 X'_t + \hat{\beta}_1$$

and applies the same kernel function employed in the first regression model (equation 2, above) to transform the instantaneous voltage time series values. Similarly to the *Model Fitting* and *Model Testing* sections of the manuscript, the result of this analysis produced, for each location, a measurement of r^2 (based on the residuals generated from comparing predicted with actual values) for each of the two models. It is worth noting that this comparison statistically slightly favored the first model, because it took advantage of two input variables (power and phase) instead of one, and because we did not separate the data into a training and a test set.

In sum, these additional analyses determined the degree to which cortical excitability can be predicted by either the instantaneous voltage or by a linear combination of power and phase.

Cortical Mapping

We used commercial Curry software (Neuroscan, El Paso, TX) or the freely available Freesurfer image analysis suite (<http://surfer.nmr.mgh.harvard.edu/>) to create subject-specific three-dimensional (3D) cortical brain models from high-resolution pre-operative magnetic resonance imaging (MRI) scans. We co-registered the MRIs with post-operative CT images using the freely available Matlab package SPM8 (<http://www.fil.ion.ucl.ac.uk/spm/>) and extracted, for each grid electrode, the stereotactic coordinates and functional area according to the Talairach atlas [74]. We used the 3D cortical template provided by the Montreal Neurological Institute (<http://www.bic.mni.mcgill.ca>) to display aggregate electrode locations from multiple subjects onto a common coordinate space, and used our NeuralAct toolbox [75] for visualization.

Results

We calculated the average model fits (r^2) across all 126 task-related locations from all 28 subjects and across the motor and auditory tasks. The average r^2 values for oscillatory power, phase, and instantaneous amplitude were 0.60, 0.55, and 0.72, respectively (see Fig. 4). Statistical analyses confirmed that the instantaneous voltage of biased oscillations is a better predictor of cortical excitability than either oscillatory power or phase (paired Wilcoxon Signed Rank tests; $p < 0.01$). Moreover, the bias-correction is critical for this improvement: when we did not re-introduce the amplitude bias into the data and rather

simply used bandpass-filtered oscillatory amplitude, the same analysis only gave an r^2 value of 0.49 (as compared to 0.72 when we did re-introduce that bias; $p < 0.001$ when comparing alpha band pass to envelope, or alpha band pass to phase, Wilcoxon signed rank tests).

We also determined the distribution of r^2 values for both the model that incorporated the amplitude envelope and phase as well as the model that incorporated just the instantaneous amplitude. The results demonstrate that the predictions of excitability produced by envelope and phase together were statistically indistinguishable from those produced by the instantaneous amplitude alone ($p \gg 0.05$, Mann-Whitney U test)¹¹. We also established (using a test for Type II errors in two-tailed tests of population mean with unknown variance) that it was unlikely ($p < 0.001$) that we failed to detect an actual difference between these conditions. Finally, we determined that submitting a randomly selected subset of non-task-related locations to the same analysis ($n = 144$ control locations, i.e., the same number of task-related locations submitted to our primary analyses) again demonstrated that models including power and phase together could not outperform models including only the biased instantaneous voltage of alpha oscillations ($p = 0.55$, Mann-Whitney U test).

We considered the possibility that the principal results described here may have been supported by the choice of binning or modeling approaches, a few exemplary channels, a few exemplary subjects, by only one of the two tasks, or by our particular filtering procedure. The following sections demonstrate the results from additional analyses that establish that this was not the case.

Control Analyses

Results were not affected by the number of bins chosen for analysis—For our primary analyses, we binned broadband gamma envelope values into 100 bins according to power, phase, or instantaneous voltage. This binning procedure has the advantage that the distribution of samples can be equalized across the value range. We then reported goodness-of-fit metrics (r^2 s) for each of these three measurements in each task-related channel. The number of bins affects the r^2 values, because it affects the number of data points that will be averaged within each bin (and hence the expected variance of the average within each bin). While we did not expect that this would preferentially benefit either the power, phase, or voltage measurement, we still evaluated the effect of using different numbers of bins (100, 500, 1000, or 2000) on the results. These control analyses are reported in Table 1 and show that using a different number of bins did not affect our conclusions.

Results were not affected by the binning procedure

The binning procedure that we used in our main analyses allowed us to equalize the number of samples within the bins. We did not have a reason to believe that this binning procedure may preferentially bias one method over another, but to exclude this possibility, we executed the same procedure on the raw data samples, i.e., without binning them across the different measurements of oscillatory activity. The results show that the instantaneous amplitude was

¹¹This conclusion remained the same even when we low-pass filtered the gamma envelope at 12 Hz to limit its rate of temporal variability to that of alpha oscillations.

still better than both the power and the phase measurements ($p < 0.05$ and $p \ll 0.05$, respectively, paired Wilcoxon signed rank test).

Results were not affected by the choice of model to fit

To test the relationship between oscillatory power, phase, or instantaneous voltage and broadband gamma, we chose models that were motivated by preliminary observations and the literature to fit our data. Specifically, we chose a sigmoid function to model power and instantaneous voltage, and a cosine function to model phase.

It is possible that the application of different types of models would change our conclusions. Our results show that this was not the case. Specifically, we recomputed our results using a linear fit for power and instantaneous voltage and a circular-linear fit for phase. Regardless of model choice, instantaneous voltage was the best predictor of cortical excitability as assessed by r^2 model fits (Table 1).

To completely eliminate any bias that could be introduced by model choice or assumptions of linearity, we also applied non-parametric Spearman correlations or non-parametric circular-linear correlations to all data points. The results again confirmed that instantaneous voltage was the best predictor of cortical excitability ($p < 0.05$ for instantaneous voltage versus envelope; and $p \ll 0.01$ for instantaneous voltage versus phase, Wilcoxon signed rank tests).

Results were not driven by a few exemplary channels or subjects, or by one task

It is possible that our results were driven by a few exemplary channels. Our results suggest that this was not the case: of all 126 electrodes included in our analyses, the majority (100, 79%) showed instantaneous alpha voltage to be the best predictor of cortical excitability (i.e., r^2 s for the instantaneous voltage were higher than the r^2 s for alpha power and phase, respectively). It is unlikely that this result was due to chance alone ($p \ll 0.01$, two-tailed Chi-Squared test).

Furthermore, we separated channels by task modality (auditory or motor), and found similar results: for 64 of the 82 (78%) motor channels, and for 36 of the 44 (82%) auditory channels, instantaneous alpha voltage was the best predictor of cortical excitability ($p \ll 0.01$ and $p \ll 0.01$, respectively).

Finally, we conclude that these results were not driven by one or a few exemplary subjects; an average (median) of 81.7% of locations in each subject had a better fit for instantaneous voltage than for power or phase (95% confidence intervals: 63.4%–88.5%). Performing this analysis on each task separately shows the same tendency (a median of 84.5% in motor locations; 95% confidence interval: 62.8%–90.0%; a median of 100.0% in auditory locations; 95% confidence interval: 67.2%–100.0%).

Results were not affected by the filtering procedure

We used an IIR filter to extract oscillatory activity in our primary analyses. The use of an FIR filter produced very similar results ($r^2 = 0.62, 0.58$, and 0.74 (power, phase, and instantaneous amplitude, respectively)), and did not change our conclusions.

Discussion

Since the introduction of computer-based quantitative analyses, power and phase measurements have been the dominant features of oscillatory brain activity. The recently proposed Function-through-Biased-Oscillations (FBO) hypothesis [1] synthesized the traditionally separate power- and phase-based views into an alternative: oscillatory activity may be best understood as repetitive modulations that drive the cortical surface potential from a low (excitatory) resting voltage towards a higher (inhibitory) voltage. This view introduced a link between oscillatory activity and its physiological origin, and synthesized the previous suggestion of rhythmic inhibitory pulsing [62, 58] with initial experimental observations that suggested the presence of a voltage asymmetry in oscillatory activity [59, 60]. This alternative view directly implies that the new and alternative measurement of the instantaneous voltage of oscillatory activity should better predict cortical excitability compared to the more traditional measurements of power or phase. We tested this central prediction in a large ECoG-based study using data from 28 subjects.

Our analyses confirmed the results from many previous studies by showing that cortical excitability (as indexed in our study by its proxy, broadband gamma) is related to oscillatory power ($r^2 = 0.60$) and oscillatory phase ($r^2 = 0.55$). Critically, they show that cortical excitability is better explained by the instantaneous amplitude of biased oscillations ($r^2 = 0.72$), and that the precision of the predictions of cortical excitability made by oscillatory power and phase together did not exceed those of the instantaneous amplitude. Multiple control analyses lessened the possibility that these findings could be described by alternative explanations including reliance on effects present in only a subset of the data. These results confirm the most central prediction of the FBO hypothesis and support a view of rhythmic inhibitory modulation of the cortex whose moment-by-moment effect on cortical excitability can be best described by the instantaneous oscillatory voltage amplitude. See Fig. 5 for an example that illustrates how cortical excitation (as measured by broadband gamma) can be high during periods of high oscillatory power, and how it can be continually high across peaks and troughs of oscillatory activity when oscillatory power is low.

The introduction of instantaneous amplitude as a measurement of cortical excitability does not negate the ability of the nervous system to separately vary oscillatory power (primarily to exert top-down control) or phase (i.e., phase resetting, to allow for bottom-up influences) to achieve variations in cortical excitability [1]. Thus, the testing of certain hypotheses (e.g., how a particular stimulus affects phase resetting in supramodal cortices) will require the separate evaluation of task-related effects on the constituent measurements of power or phase.

The finding that instantaneous voltage regulates cortical excitability has principal implications for the interpretation of previous and future experimental studies of oscillatory activity, because it offers an alternative measurement that is more physiologically motivated, simpler, and more explanatory of cortical excitability. It also has central implications for the interpretation of measurements that are derived from oscillatory power or phase. For example, measurements of phase-amplitude-coupling (PAC) are often used to quantify the effects of specific tasks on neural signals. However, the view that is reinforced by the present

study suggests that the relationship between oscillatory activity and cortical population-level activity may represent a (relatively fixed) physiological principle rather than yet another variable control mechanism¹². If this is correct, complex measurements derived from oscillatory or cortical activity, such as PAC, cross-frequency coupling, or amplitude-amplitude coupling, may simply be explained by changes in their constituent variables.

The introduction of the instantaneous voltage amplitude as an alternative measurement may also benefit future basic or applied neuroscientific studies. Because it provides an accurate measurement of cortical excitability, the use of instantaneous amplitude may help to detect smaller effect sizes. Furthermore, because scalp-recorded EEG data is much more prevalent than ECoG data, the significance of this metric will be enhanced if the present findings can be replicated with EEG. In this case, the function of the large number of clinical applications supported by scalp-recorded EEG (brain-computer interfaces (BCIs) that aim to restore function lost by devastating neurological disorders, or diagnostic devices such as depth-of-anesthesia monitors) could be improved by introducing a simple change to the feature extraction component of the signal processing framework, i.e., without any changes to sensing or recording hardware.

In our study, we evaluated the relationship between different measurements of oscillatory activity in the alpha band and broadband gamma activity in motor and auditory cortical areas. Because this relationship appears to be relatively general and can be found for other low-frequency bands and other cortical locations (e.g., theta oscillations and the hippocampus [77]), it is possible that the findings from our present study may generalize as well.

Finally, and in particular if the results demonstrated here can be shown to represent a general phenomenon, our findings have fundamental implications on existing theories of cortical information transmission. Specifically, Communication-Through-Coherence (CTC, [78]) proposed that information across cortical sites is facilitated by oscillatory phase synchrony across these sites. In contrast, Gating-By-Inhibition (GBI, [34]) proposed that cortical information processing is facilitated/inhibited at each location through modulation of oscillatory power. Because the present study supports the fusion of the concepts of oscillatory power and phase, it suggests that the principles of cortical information transmission may alternatively be understood by a model that expands on and synthesizes CTC and GBI, as proposed in [1].

While the present results are encouraging, many questions currently remain unanswered. These questions include the empirical prevalence and other properties of asymmetric voltage distributions in the data, and the impact of the instantaneous voltage on important characteristics of cortical information transmission. Proper resolution of these questions should provide important new insights into the dynamic modulation of cortical function.

¹²We are aware that changes in PAC can be associated with particular disorders such as Parkinson's Disease [76].

Acknowledgments

We are grateful for critical comments by Peter Brunner, Arnaud Delorme, Sivylla Paraskevopoulou, and Adriana de Pestors. This work was supported by the NIH (R01-EB00856, R01-EB006356, P41-EB018783, and R37-NS21135), the US Army Research Office (W911NF-08-1-0216, W911NF-12-1-0109, W911NF-14-1-0440) and Fondazione Neurone. G.S. designed the study. W.G.C. and J.M. analyzed data. G.S., R.T.K., and W.G.C. wrote the paper. All authors discussed results.

References

- Schalk G. A general framework for dynamic cortical function: the function-through-biased-oscillations (fbo) hypothesis. *Frontiers in Human Neuroscience*. 9(352)
- Bishop GH. Cyclic changes in excitability of the optic pathway of the rabbit. *American Journal of Physiology*. 1932; 103(1):213–224.
- Bollimunta A, Mo J, Schroeder CE, Ding M. Neuronal mechanisms and attentional modulation of corticothalamic alpha oscillations. *The Journal of Neuroscience*. 2011; 31(13):4935–4943. [PubMed: 21451032]
- Saalmann YB, Pinsk MA, Wang L, Li X, Kastner S. The pulvinar regulates information transmission between cortical areas based on attention demands. *Science*. 2012; 337(6095):753–756. [PubMed: 22879517]
- Costa MS, Born J, Claussen JC, Martinetz T. Modeling the effect of sleep regulation on a neural mass model. *Journal of computational neuroscience*. 2016; 41(1):15–28. DOI: 10.1007/s10827-016-0602-z [PubMed: 27066796]
- Singer W, Gray CM. Visual feature integration and the temporal correlation hypothesis. *Annu Rev Neurosci*. 1995; 18(1):555–586. [PubMed: 7605074]
- Miltner WH, Braun C, Arnold M, Witte H, Taub E. Coherence of gamma-band EEG activity as a basis for associative learning. *Nature*. 1999; 397(6718):434–436. [PubMed: 9989409]
- Sauseng P, Klimesch W, Heise KF, Gruber WR, Holz E, Karim AA, Glennon M, Gerloff C, Birbaumer N, Hummel FC. Brain oscillatory substrates of visual short-term memory capacity. *Current Biology*. 2009; 19(21):1846–1852. [PubMed: 19913428]
- Canolty RT, Edwards E, Dalal SS, Soltani M, Nagarajan SS, Kirsch HE, Berger MS, Barbaro NM, Knight RT. High gamma power is phase-locked to theta oscillations in human neocortex. *Science*. 2006; 313(5793):1626–1628. DOI: 10.1126/science.1128115 [PubMed: 16973878]
- Siapas AG, Lubenov EV, Wilson MA. Prefrontal phase locking to hippocampal theta oscillations. *Neuron*. 2005; 46(1):141–151. [PubMed: 15820700]
- Sederberg PB, Kahana MJ, Howard MW, Donner EJ, Madsen JR. Theta and gamma oscillations during encoding predict subsequent recall. *J Neurosci*. 2003; 23(34):10809–10814. [PubMed: 14645473]
- Fitzgibbon SP, Pope KJ, Mackenzie L, Clark CR, Willoughby JO. Cognitive tasks augment gamma EEG power. *Clin Neurophysiol*. 2004; 115(8):1802–1809. [PubMed: 15261859]
- Howard MW, Rizzuto DS, Caplan JB, Madsen JR, Lisman J, Aschenbrenner-Scheibe R, Schulze-Bonhage A, Kahana MJ. Gamma oscillations correlate with working memory load in humans. *Cereb Cortex*. 2003; 13(12):1369–1374. [PubMed: 14615302]
- Womelsdorf T, Fries P, Mitra PP, Desimone R. Gamma-band synchronization in visual cortex predicts speed of change detection. *Nature*. 2006; 439(7077):733–736. [PubMed: 16372022]
- Haegens S, Nácher V, Luna R, Romo R, Jensen O. α -oscillations in the monkey sensorimotor network influence discrimination performance by rhythmical inhibition of neuronal spiking. *Proceedings of the National Academy of Sciences*. 2011; 108(48):19377–19382.
- Kubaneck J, Snyder LH, Brunton BW, Brody CD, Schalk G. A low-frequency oscillatory neural signal in humans encodes a developing decision variable. *NeuroImage*. 2013; 83:795–808. [PubMed: 23872495]
- Kubaneck J, Hill NJ, Snyder LH, Schalk G. Cortical alpha activity predicts the confidence in an impending action. *Front Neurosci*. 9

18. Szczepanski SM, Crone NE, Kuperman RA, Auguste KI, Parvizi J, Knight RT. Dynamic changes in phase-amplitude coupling facilitate spatial attention control in fronto-parietal cortex. *PLoS Biol.* 2014; 12:e1001936. [PubMed: 25157678]
19. L. rincz ML, Kékesi KA, Juhász G, Crunelli V, Hughes SW. Temporal framing of thalamic relay-mode firing by phasic inhibition during the alpha rhythm. *Neuron.* 2009; 63(5):683–696. [PubMed: 19755110]
20. Reimer J, Hatsopoulos NG. Periodicity and evoked responses in motor cortex. *The Journal of Neuroscience: the official journal of the Society for Neuroscience.* 2010; 30(34):11506–11515. DOI: 10.1523/JNEUROSCI.5947-09.2010 [PubMed: 20739573]
21. Takahashi K, Kim S, Coleman TP, Brown KA, Suminski AJ, Best MD, Hatsopoulos NG. Large-scale spatiotemporal spike patterning consistent with wave propagation in motor cortex. *Nature Communications.* 2015; 6:7169.doi: 10.1038/ncomms8169
22. Fries P, Reynolds JH, Rorie AE, Desimone R. Modulation of oscillatory neuronal synchronization by selective visual attention. *Science (New York, NY).* 2001; 291(5508):1560–1563. DOI: 10.1126/science.291.5508.1560
23. Fries P, Neuenschwander S, Engel AK, Goebel R, Singer W. Rapid feature selective neuronal synchronization through correlated latency shifting. *Nature Neuroscience.* 2001; 4(2):194–200. DOI: 10.1038/84032 [PubMed: 11175881]
24. Voytek B, Canolty RT, Shestyuk A, Crone N, Parvizi J, Knight RT. Shifts in gamma phase-amplitude coupling frequency from theta to alpha over posterior cortex during visual tasks. *Front Hum Neurosci.* 4(191)
25. Miller KJ, Hermes D, Honey CJ, Hebb AO, Ramsey NF, Knight RT, Ojemann JG, Fetz EE. Human motor cortical activity is selectively phase-entrained on underlying rhythms. *PLoS Computational Biology.* 2012; 8(9):e1002655.doi: 10.1371/journal.pcbi.1002655 [PubMed: 22969416]
26. Pfurtscheller G, Neuper C. Simultaneous eeg 10 hz desynchronization and 40 hz synchronization during finger movements. *NeuroReport.* 1992; 3(12):1057–1060. [PubMed: 1493217]
27. Crone NE, Boatman D, Gordon B, Hao L. Induced electrocorticographic gamma activity during auditory perception. *J Clin Neurophysiol.* 2001; 112(4):565–582.
28. Potes C, Brunner P, Gunduz A, Knight RT, Schalk G. Spatial and temporal relationships of electrocorticographic alpha and gamma activity during auditory processing. *NeuroImage.* 2014; 97:188–195. [PubMed: 24768933]
29. Romei V, Gross J, Thut G. On the role of prestimulus alpha rhythms over occipito-parietal areas in visual input regulation: correlation or causation? *The Journal of Neuroscience.* 2010; 30(25):8692–8697. [PubMed: 20573914]
30. Mazaheri A, van Schouwenburg MR, Dimitrijevic A, Denys D, Cools R, Jensen O. Region-specific modulations in oscillatory alpha activity serve to facilitate processing in the visual and auditory modalities. *NeuroImage.* 2014; 87:356–362. [PubMed: 24188814]
31. Coon WG, Gunduz A, Brunner P, Ritaccio AL, Pesaran B, Schalk G. Oscillatory phase modulates the timing of neuronal activations and resulting behavior. *NeuroImage.* 2016; 133:294–301. DOI: 10.1016/j.neuroimage.2016.02.080 [PubMed: 26975551]
32. de Pestiers A, Coon WG, Brunner P, Gunduz A, Ritaccio AL, Brunet NM, de Weerd P, Roberts MJ, Oostenveld R, Fries P, Schalk G. Alpha power indexes task-related networks on large and small scales: A multimodal ecog study in humans and a non-human primate. *NeuroImage.* 2016; 134:122–131. DOI: 10.1016/j.neuroimage.2016.03.074 [PubMed: 27057960]
33. Fries P. A mechanism for cognitive dynamics: neuronal communication through coherence. *Trends Cogn Sci.* 2005; 9(10):474–480. [PubMed: 16150631]
34. Jensen O, Mazaheri A. Shaping functional architecture by oscillatory alpha activity: gating by inhibition. *Front Hum Neurosci.* 2010; 4:186.doi: 10.3389/fnhum.2010.00186 [PubMed: 21119777]
35. Schalk G. A general framework for dynamic cortical function: the function-through-biased-oscillations (FBO) hypothesis. *Front Hum Neurosci.* 9
36. Voytek B, Secundo L, Bidet-Caulet A, Scabini D, Stiver SI, Gean AD, Manley GT, Knight RT. Hemispherectomy: a new model for human electrophysiology with high spatio-temporal resolution. *J Cogn Neurosci.* 2010; 22(11):2491–2502. [PubMed: 19925193]

37. Darvas F, Scherer R, Ojemann JG, Rao R, Miller KJ, Sorensen LB. High gamma mapping using EEG. *NeuroImage*. 2010; 49(1):930–938. [PubMed: 19715762]
38. Edwards E, Nagarajan SS, Dalal SS, Canolty RT, Kirsch HE, Barbaro NM, Knight RT. Spatiotemporal imaging of cortical activation during verb generation and picture naming. *NeuroImage*. 2010; 50(1):291–301. [PubMed: 20026224]
39. Edwards E, Soltani M, Deouell LY, Berger MS, Knight RT. High gamma activity in response to deviant auditory stimuli recorded directly from human cortex. *J Neurophysiol*. 2005; 94(6):4269–4280. [PubMed: 16093343]
40. Edwards E, Soltani M, Kim W, Dalal SS, Nagarajan SS, Berger MS, Knight RT. Comparison of time-frequency responses and the event-related potential to auditory speech stimuli in human cortex. *J Neurophysiol*. 2009; 102(1):377–386. [PubMed: 19439673]
41. Chang EF, Edwards E, Nagarajan SS, Fogelson N, Dalal SS, Canolty RT, Kirsch HE, Barbaro NM, Knight RT. Cortical spatio-temporal dynamics underlying phonological target detection in humans. *J Cogn Neurosci*. 2011; 23(6):1437–1446. [PubMed: 20465359]
42. Jensen O, Kaiser J, Lachaux JP. Human gamma-frequency oscillations associated with attention and memory. *Trends Neurosci*. 2007; 30(7):317–324. [PubMed: 17499860]
43. Maris E, van Vugt M, Kahana M. Spatially distributed patterns of oscillatory coupling between high-frequency amplitudes and low-frequency phases in human iEEG. *NeuroImage*. 2011; 54(2):836–850. [PubMed: 20851192]
44. Ray S, Niebur E, Hsiao SS, Sinai A, Crone NE. High-frequency gamma activity (80–150 Hz) is increased in human cortex during selective attention. *Clin Neurophysiol*. 2008; 119(1):116–133. [PubMed: 18037343]
45. Tort AB, Kramer MA, Thorn C, Gibson DJ, Kubota Y, Graybiel AM, Kopell NJ. Dynamic cross-frequency couplings of local field potential oscillations in rat striatum and hippocampus during performance of a t-maze task. *Proc Natl Acad Sci U S A*. 2008; 105(51):20517–20522. [PubMed: 19074268]
46. Wang W, Collinger JL, Perez MA, Tyler-Kabara EC, Cohen LG, Birbaumer N, Brose SW, Schwartz AB, Boninger ML, Weber DJ. Neural interface technology for rehabilitation: exploiting and promoting neuroplasticity. *Phys Med Rehabil Clin N Am*. 2010; 21(1):157–178. DOI: 10.1016/j.pmr.2009.07.003 [PubMed: 19951784]
47. Miller KJ, Sorensen LB, Ojemann JG, den Nijs M. Power-law scaling in the brain surface electric potential. *PLoS Comput Biol*. 2009; 5(12):e1000609.doi: 10.1371/journal.pcbi.1000609 [PubMed: 20019800]
48. Whittingstall K, Logothetis NK. Frequency-band coupling in surface eeg reflects spiking activity in monkey visual cortex. *Neuron*. 2009; 64(2):281–289. [PubMed: 19874794]
49. Manning JR, Jacobs J, Fried I, Kahana MJ. Broadband shifts in local field potential power spectra are correlated with single-neuron spiking in humans. *J Neurosci*. 2009; 29(43):13613–13620. [PubMed: 19864573]
50. Ray S, Maunsell JH. Different origins of gamma rhythm and high-gamma activity in macaque visual cortex. *PLoS Biology*. 2011; 9(4):e1000610. [PubMed: 21532743]
51. Logothetis NK, Pauls J, Augath M, Trinath T, Oeltermann A. Neurophysiological investigation of the basis of the fMRI signal. *Nature*. 2001; 412(6843):150–157. [PubMed: 11449264]
52. Mukamel R, Gelbard H, Arieli A, Hasson U, Fried I, Malach R. Coupling between neuronal firing, field potentials, and fMRI in human auditory cortex. *Science*. 2005; 309(5736):951–954. [PubMed: 16081741]
53. Niessing J, Ebisch B, Schmidt KE, Niessing M, Singer W, Galuske RA. Hemodynamic signals correlate tightly with synchronized gamma oscillations. *Science*. 2005; 309(5736):948–951. [PubMed: 16081740]
54. Engell AD, Huettel S, McCarthy G. The fMRI BOLD signal tracks electrophysiological spectral perturbations, not event-related potentials. *NeuroImage*. 2012; 59(3):2600–2606. [PubMed: 21925278]
55. Jasper H, Penfield W. Electrocorticograms in man: effect of voluntary movement upon the electrical activity of the precentral gyrus. *Archiv für Psychiatrie und Nervenkrankheiten*. 1949; 183(1–2):163–174.

56. Pfurtscheller G. Functional topography during sensorimotor activation studied with event-related desynchronization mapping. *Journal of Clinical Neurophysiology*. 1989; 6(1):75–84. [PubMed: 2915031]
57. Krusienski DJ, Schalk G, McFarland DJ, Wolpaw JR. A-rhythm matched filter for continuous control of a brain-computer interface, *Biomedical Engineering. IEEE Transactions on*. 2007; 54(2):273–280.
58. Mazaheri A, Jensen O. Rhythmic pulsing: linking ongoing brain activity with evoked responses. *Front Hum Neurosci*. 4
59. Mazaheri A, Jensen O. Asymmetric amplitude modulations of brain oscillations generate slow evoked responses. *The Journal of Neuroscience*. 2008; 28(31):7781–7787. [PubMed: 18667610]
60. Nikulin VV, Linkenkaer-Hansen K, Nolte G, Curio G. Non-zero mean and asymmetry of neuronal oscillations have different implications for evoked responses. *Clinical Neurophysiology*. 2010; 121(2):186–193. [PubMed: 19914864]
61. Li CL. The inhibitory effect of stimulation of a thalamic nucleus on neuronal activity in the motor cortex. *The Journal of Physiology*. 1956; 133(1):40. [PubMed: 13346633]
62. Klimesch W, Sauseng P, Hanslmayr S. Eeg alpha oscillations: the inhibition–timing hypothesis. *Brain Research Reviews*. 2007; 53(1):63–88. [PubMed: 16887192]
63. Schalk G, McFarland DJ, Hinterberger T, Birbaumer N, Wolpaw JR. BCI2000: a general-purpose brain-computer interface (BCI) system. *IEEE Trans Biomed Eng*. 2004; 51(6):1034–1043. [PubMed: 15188875]
64. Schalk, G., Mellinger, J. *A Practical Guide to Brain–Computer Interfacing with BCI2000*. Springer; New York: 2010.
65. Gunduz A, Brunner P, Daitch A, Leuthardt EC, Ritaccio AL, Pesaran B, Schalk G. Neural correlates of visual–spatial attention in electrocorticographic signals in humans. *Front Hum Neurosci*. 2011; 5:89. [PubMed: 22046153]
66. Gunduz A, Brunner P, Daitch A, Leuthardt EC, Ritaccio AL, Pesaran B, Schalk G. Decoding covert spatial attention using electrocorticographic (ecog) signals in humans. *NeuroImage*. 2012; 60(4):2285–2293. DOI: 10.1016/j.neuroimage.2012.02.017 [PubMed: 22366333]
67. Pei X, Leuthardt EC, Gaona CM, Brunner P, Wolpaw JR, Schalk G. Spatiotemporal dynamics of electrocorticographic high gamma activity during overt and covert word repetition. *NeuroImage*. 2011; 54(4):2960–2972. [PubMed: 21029784]
68. Miller KJ, Sorensen LB, Ojemann JG, Den Nijs M. Power-law scaling in the brain surface electric potential. *PLoS Comput Biol*. 2009; 5(12):e1000609. [PubMed: 20019800]
69. Liu Y, Coon W, de Pestors A, Brunner P, Schalk G. The effects of spatial filtering and artifacts on electrocorticographic signals. *Journal of Neural Engineering*. 2015; 12(5):056008. [PubMed: 26268446]
70. Crone NE, Sinai A, Korzeniewska A. High-frequency gamma oscillations and human brain mapping with electrocorticography. *Progress in Brain Research*. 2006; 159:275–295. [PubMed: 17071238]
71. Womelsdorf T, Schoffelen JM, Oostenveld R, Singer W, Desimone R, Engel AK, Fries P. Modulation of neuronal interactions through neuronal synchronization. *Science (New York, NY)*. 2007; 316(5831):1609–1612. DOI: 10.1126/science.1139597
72. Siegel M, Warden MR, Miller EK. Phase-dependent neuronal coding of objects in short-term memory. *Proceedings of the National Academy of Sciences*. 2009; 106(50):21341–21346.
73. Sarma Y, Jammalamadaka S. Circular regression. *Statistical Science and Data Analysis*. 1993:109–128.
74. Lancaster JL, Woldorff MG, Parsons LM, Liotti M, Freitas CS, Rainey L, Kochunov PV, Nickerson D, Mikiten SA, Fox PT. Automated Talairach atlas labels for functional brain mapping. *Hum Brain Mapp*. 2000; 10(3):120–131. [PubMed: 10912591]
75. Kubanek J, Schalk G. NeuralAct: a tool to visualize electrocortical (ECoG) activity on a three-dimensional model of the cortex. *Neuroinformatics*. 2014:1–8. [PubMed: 24174261]
76. De Hemptinne C, Ryapolova-Webb ES, Air EL, Garcia PA, Miller KJ, Ojemann JG, Ostrem JL, Galifianakis NB, Starr PA. Exaggerated phase–amplitude coupling in the primary motor cortex in parkinson disease. *Proceedings of the National Academy of Sciences*. 2013; 110(12):4780–4785.

77. Lega B, Burke J, Jacobs J, Kahana MJ. Slow-theta-to-gamma phase–amplitude coupling in human hippocampus supports the formation of new episodic memories. *Cerebral Cortex*. 2014:bhu232.
78. Fries P. A mechanism for cognitive dynamics: neuronal communication through neuronal coherence. *Trends Cogn Sci*. 2005; 9(10):474–480. DOI: 10.1016/j.tics.2005.08.011 [PubMed: 16150631]

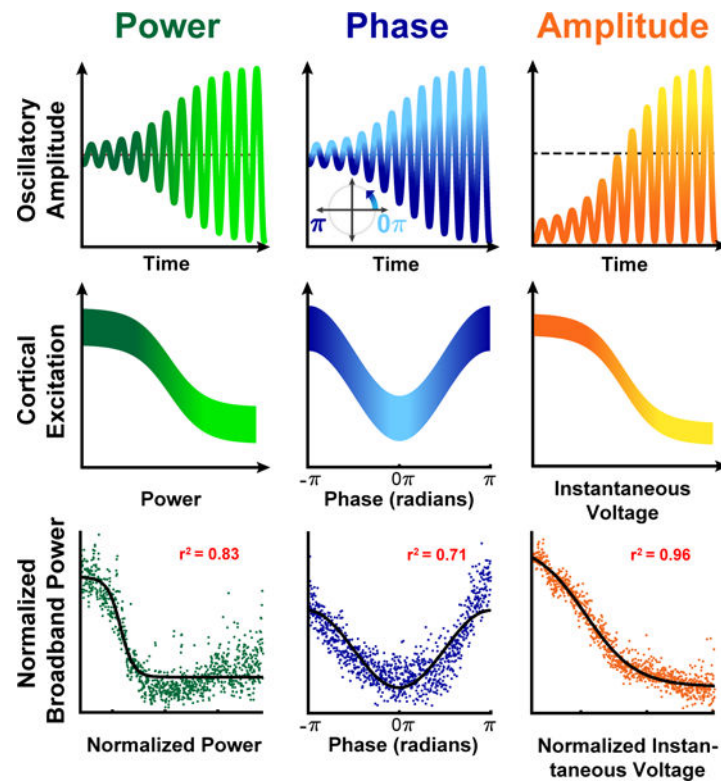


Figure 1.

Comparison of the three measurements of oscillatory power, phase, and instantaneous amplitude, their relationship to cortical excitation, and exemplary experimental data from one location. **Top row:** Left and center panels show exemplary waveforms of band-pass filtered oscillatory activity with zero mean as implied by traditional measurements of oscillatory power and phase, respectively. Right panel shows exemplary waveforms of asymmetric oscillatory activity as proposed by the FBO hypothesis. Y axes give signal amplitude; X axes give time. Color gradients indicate each measurement's theoretical relationship to cortical excitability: darker colors correspond to high excitability, and light colors correspond to low excitability. E.g., the left part of the green trace has low oscillatory power and is associated with high cortical excitability as indicated by the dark green color. **Middle Row:** Each measurement's relationship with cortical excitation (y-axis). Color gradients correspond to those in the top row. Left panel: cortical excitability (dark green color) and resulting excitation (value on y-axis) are high when oscillatory power is low. Center panel: cortical excitation and excitability are high when the oscillation is at its trough (i.e., $\pm\pi$). Right panel: cortical excitation and excitability are high when the instantaneous voltage is low. **Bottom Row:** Exemplary experimental data from one ECoG location. Each dot gives the average normalized broadband power within one of 1000 bins that are spaced linearly across each of the three X axes. These data, and their parametric fits using sigmoid/cosine functions, conform to expectations illustrated in the middle row. Y-axes give normalized broadband activity (an index of cortical excitation and a proxy for cortical excitability). In this exemplary channel, the fit (assessed as r^2) of the model to the data is 0.83 for power, 0.71 for phase, and 0.96 for instantaneous voltage.

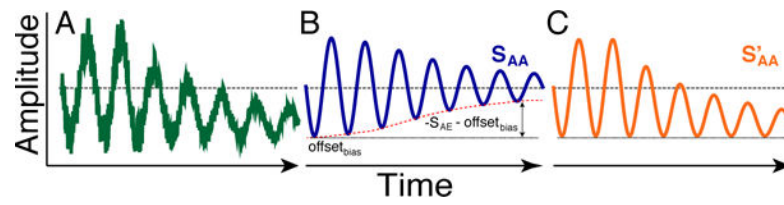


Figure 2. Extraction of the instantaneous voltage

(A) gives the time course of a simulated rhythmic signal contaminated by non-rhythmic noise. (B) gives the result of bandpass filtering the signal shown in (A). This procedure removed noise, but also removed the bias in the data and made the signal zero-mean. (C) shows the result after adding the bias back into the data. Troughs are at the same amplitude throughout.

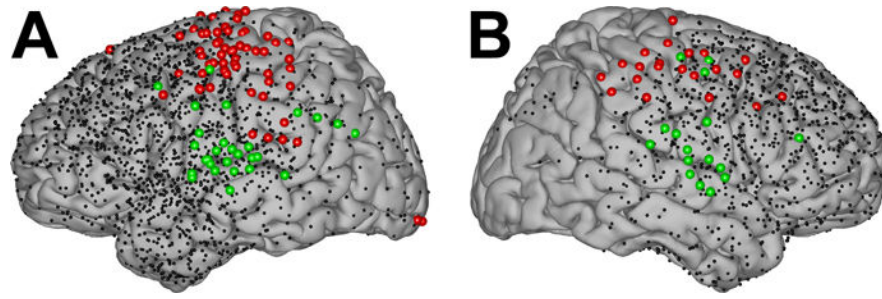


Figure 3. Electrode locations from all 28 subjects

Left (A) and right (B) hemispheres are shown. Electrodes are projected onto the common MNI template for ease of visualization. Red/green dots indicate locations whose broadband gamma activity was modulated by the motor/auditory task, respectively. Small black dots show electrode locations not related to either of the two tasks.

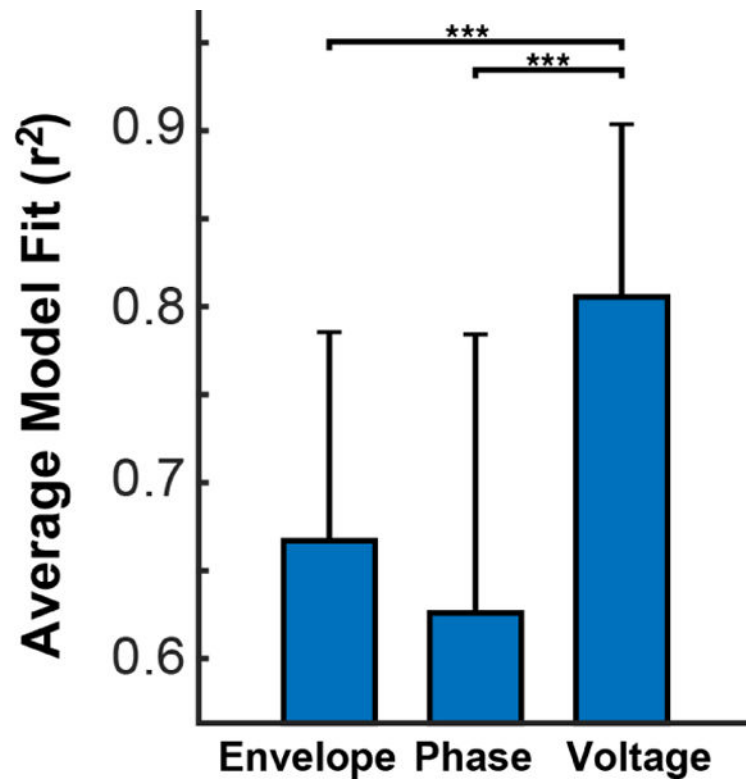


Figure 4. The instantaneous voltage of asymmetric oscillations is a better predictor of cortical excitability than either oscillatory power or phase

Y-axis gives average model fits (r^2 s) for each of the three cases. Bars give the median model fit with error bars representing the 75th percentile. *** $p < 0.001$, paired Wilcoxon Signed Rank test.

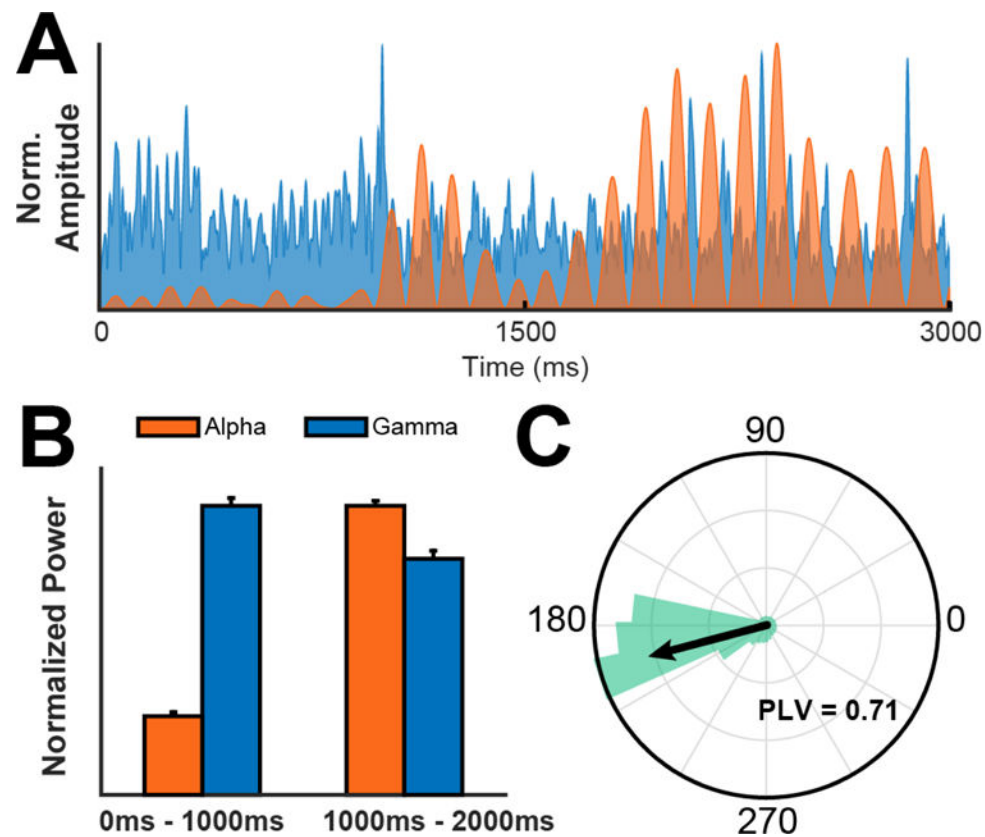


Figure 5. Oscillatory modulation of cortical activity

A. Time series of broadband gamma (shaded blue) and asymmetric (biased) alpha activity (shaded orange) in one exemplary location from one subject. **B.** Alpha power is significantly lower in the first half of A (0 – 1500ms) than in the second half (1500 – 3000ms). Concomitant changes in gamma power are consistent with a negative correlation between alpha and gamma power. **C.** When alpha power is high (e.g., 1500 – 3000ms in trace in A), broadband gamma activity becomes phase locked to the trough of alpha oscillations (phase-locking value (PLV) = 0.71; circular mean of 194.9°; $p < 0.001$, Rayleigh test for non-uniformity in circular data). No significant phase locking is observed when alpha power is low (0 – 1500ms in trace in A; PLV = 0.11; $p \gg 0.05$, Rayleigh test for non-uniformity in circular data).

Table 1
Comparison of model fits for three principle measurements — power, phase, and instantaneous voltage amplitude

Labels in left-most column delineate the number of bins across which broadband gamma values were distributed, as well as the choice of model for power and instantaneous voltage amplitude (“sigmoid” or “linear”). A cosine function with fixed cycle length and variable phase offset was always used for fitting phase data. Data in the first block shows average model fits (i.e., mean r^2 values across all 126 channels \pm standard error of the mean). Data in the block give the probability that the r^2 values produced for the two indicated measurements (e.g., power and phase) were statistically indistinguishable from each other.

Mean Model Fits (r^2)			
	Power	Phase	
100 bins sigmoid	0.60 ± 0.02	0.55 ± 0.02	0.72 ± 0.02
500 bins sigmoid	0.37 ± 0.02	0.26 ± 0.02	0.43 ± 0.02
1000 bins sigmoid	0.26 ± 0.02	0.15 ± 0.01	0.29 ± 0.02
2000 bins sigmoid	0.14 ± 0.01	0.08 ± 0.01	0.17 ± 0.01
100 bins linear	0.21 ± 0.02	0.15 ± 0.02	0.29 ± 0.02
Wilcoxon p-values			
	Wilcoxon p-values		
	Inst. Voltage vs. Power	Inst. Voltage vs. Phase	Power vs. Phase
100 bins sigmoid	0	0	0.085
500 bins sigmoid	0	0	0
1000 bins sigmoid	0	0.001	0
2000 bins sigmoid	0	0.010	0
100 bins linear	0	0	0